Proceedings of IMECE2006
2006 ASME International Mechanical Engineering Congress and Exposition
November 5-10, 2006, Chicago, Illinois, USA

IMECE2006-14416

MODELING AND TESTING OF A NEW POLYMER-BASED IMPACT TOOL DESIGN TO REDUCE NOISE, VIBRATION AND BIOMECHANICAL INJURIES

Janelle Konchar
Procter & Gamble
Cinncinatti, OH

Peter Popper
Dupont Research Fellow, Retired
Wilmington, DE

Matthew Griffith and James Glancey
University of Delaware
Newark, DE

ABSTRACT

A new power impact tool design has been developed and tested using advanced engineering polymers to replace traditional metal components. The new polymer-metal impact mechanism generates less noise, lower vibrations, and potentially reduces biomechanical injuries. Power tools are known to cause several medical ailments including Hand-Arm Vibration Syndrome (HAV), Raynaud's phenomenon, and Vibration White Finger unless the daily exposure and/or dosage is limited. To evaluate the effects of a polymer-metal impact mechanism on tool performance, a non-linear model describing the equations of motion and resulting output forces were developed. In addition, a number of experiments with a high frequency Instron test machine and prototype tools were performed to validate the model and compare performance of conventional power tools to the new polymer based design. The results show that although adding a polymer does reduce noise and vibration, the reduction in impact force is relatively small and statistically insignificant. Various polymer materials and shapes were evaluated and results show that for durability and performance, the optimum appears to be a plug inserted in a cavity in either the piston or the cutting tool, thus creating a state of confined compression on the polymer. The polymer used in this research was Minlon® (mineral reinforced Nylon66), and durability was improved when the polymer inserts were cycled with compressive loads before use in the power tool.

Keywords: power tool, impact, vibration, biomechanical injury, safety, ergonomics, engineering polymers

INTRODUCTION

Power tools have a large market presence and are valued as important pieces of equipment in industries worldwide. Traditional power tools with reciprocating impact components produce vibration energy that is transmitted to the tool user. Exposure to vibrations emitted from power impact tools represents a significant workplace hazard contributing to serious worker health problems and biomechanical injuries such as Hand-Arm Vibration Syndrome (HAVS), Vibration White Finger (VWF), and Raynaud's Phenomenon. Recent data specifies that injuries associated with hand tool operation comprised 5.2% (65,450) of the total work-related injury cases in the United States annually [1]. Out of these cases, 26.6% (17,390) involved injury resulting specifically from power hand tools [1]. Hand Arm Vibration (HAV) alone affects two million U.S. workers, with employers paying $15 billion to $20 billion a year in workers' compensation costs as a result of musculoskeletal disorders [2,3].

Long term tool use exposes workers to high levels of vibration that can cause permanent, irreversible damage to blood vessels and nerves in the hand and arm [4]. Often, hand-arm injuries are accompanied by hearing loss attributed to exposure to high vibration (and sound). In 2000, the U.S Department of Labor's Occupational Safety and Health Administration (OSHA) published ergonomics rules for all general industry employers [3]. Within this document, vibration and the use of hand tools was identified as one of five ergonomic risks factors leading to injury or symptoms for work-related musculoskeletal disorders. In March of 2001, OSHA's Ergonomics Standard was overturned by Congress,

with President George W. Bush signing the repeal of the law. This political action marked the first time in OSHA's 30-year history that an existing workplace safety and health standard was rescinded [5].

Excessive HAV exposure from vibrating pneumatic, electric, hydraulic, or gasoline-powered hand tools can produce irreversible damage to the hands [2]. As a result of the increasing ergonomic awareness and employer concern surrounding occupational vibration injury caused by the regular use of tools in the workplace, several low vibration tools have been developed, most using internal springs to reduce peak accelerations on the return stoke of a reciprocating piston [10]. Unlike previous research and development, this study has been initiated to develop a new impact tool design to reduce vibration-related biomechanical injuries using non-traditional materials to eliminate direct metal-to-metal contact and impact.

Review of Vibration Standards

The human response to vibration is not uniform or linear across the frequency spectrum. ISO 5349 specifies guidelines for vibration measurement and assessment of human exposure to hand transmitted vibration [11]. A frequency weighting curve for acceleration data (Figure 1) reflects the human body's sensitivity to hand-arm vibration exposure at lower frequencies. For HAV measurement, three perpendicular directions of vibration, illustrated in Figure 2, are measured simultaneously. The frequency weighted root mean square of these three individual axis measurements is reported as the total value of vibration.

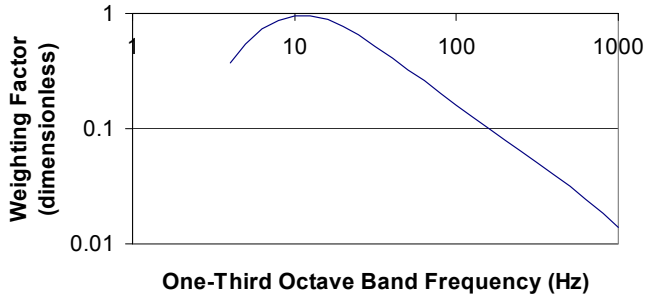

Figure 1. Frequency weighting factors for hand-transmitted vibration. (ISO 5349)

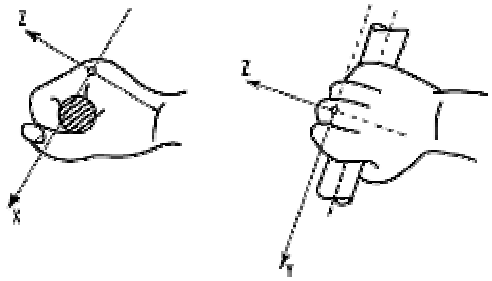

Figure 2. Tri-axial vibration measurement. (ISO 5349)

Objectives for This Study

The overall goal of this work is to improve conventional power tool designs by integrating high-performance engineering polymers as a means to reduce the potential development of harmful biomechanical ailments associated with their long-term use. Previous work has reported a methodology for characterizing and modifying the vibration behavior of commercially available tools [6, 12].

For the purpose of this study, work will focus on hand-held power impact tools with an emphasis on the design and performance of pneumatic-powered reciprocating devices. The analysis and testing described herein investigates the feasibility and performance benefits of a modified accessory chisel that includes a polymer insert. First, a simple mass-spring analog is developed to obtain the governing equations of motion of the piston-chisel system. This mathematical model allows for the assessment of the force transmission characteristics of chisels for different insert materials in order to develop material property requirements to select a suitable high-performance reinforced polymer. Second, laboratory experiments are performed using a hydraulic testing machine to measure polymer integrity for prototype chisels as a function of the number of impacts (i.e. loading cycles). Third, field (human) testing is conducted to measure vibration and noise from conventional and modified power tools to quantify potential biomechanical benefits of vibration and sound reduction to the tool user.

CONCEPTUAL DEVELOPMENT

Mechanics of the Pneumatic Impact Tool

A simple schematic of a pneumatic impact tool system powered by compressed air is shown in Figure 3. The benchmark tool analyzed in this study was a Dayton Model 2Z486C Medium Duty Air Hammer rated at 3000 blows per minute for a 90 psi supply pressure (Figure 4). When the trigger is pulled a valve in the tool chamber opens, allowing air pressure to be applied to the back of the piston. During the stroke of the piston, the relative location of air passages with respect to piston position changes, causing the oscillatory nature of the piston motion. Placement of these air passages allows air to flow in one direction during the piston down stroke, and air to flow in the opposite direction during piston reversal. As the piston reaches maximum allowable stroke length within the tool cylinder, impact occurs between the front of the reciprocating piston and the top end of the steel chisel, extending the chisel for cutting into the desired "work". A safety retainer keeps the chisel seated against the chamber and prevents the chisel accessory from ejection during tool operation.

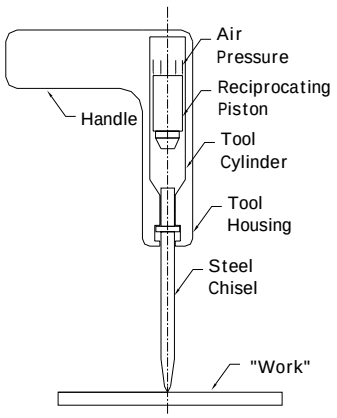

Figure 3. Conceptual view of a pneumatic impact chisel.

Figure 4. A Dayton Model ZZ486C pneumatic impact chisel.

Design Considerations for Low Vibration and Sound

The impact between the steel piston and steel chisel is a principle source of vibration generated by the tool system. By integrating engineering polymers into current power tool designs, the direct metal-to-metal contact between the piston and chisel components can be eliminated. The ambition of this material substitution, to dissipate the overall vibration magnitude and remove harmful frequencies of vibration transmitted to the hand and arm extremities, represents a significant improvement in the safety of conventional tool systems. Furthermore, this ergonomic performance enhancement must be achieved without compromising the cutting performance of the power tool.

Screening experiments to assess the feasibility, key design issues and potential advantages of integrating polymers into power tool design, were performed by modifying the piston component. Modified steel pistons were adapted into two prototype treatments, one incorporating polymer material at the front impact end of the piston while the second concept added polymer material to the back surface of the piston (Figure 5). To accommodate a front insert, a hole was drilled into the piston allowing a cylindrical polymer insert to be pressed (interference fit) into the cavity created from the removed steel material. The back insert configuration required no additional

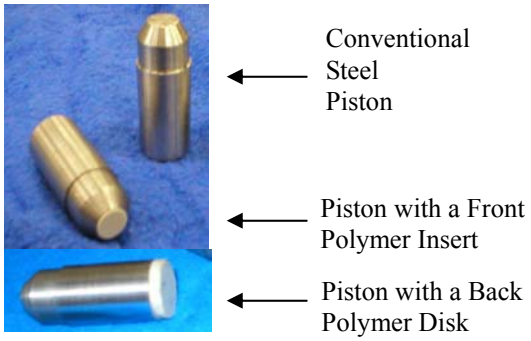

Figure 5. Modified pistons used for proof of concept testing.

machining to the duplicate piston; a two part epoxy with a thermosetting resin (rated tensile strength 3960 psi and rated tensile lap shear 1040 psi) was used to bond a 3 mm thick circular polymer disk to the rear piston face.

Sound level measurements provided supporting data that substantiated perceived vibration attenuation. Two trials were conducted for each piston treatment, with microphone location 1 meter from the power tool and a data acquisition sampling frequency of 60 kHz. Table 1 summarizes the results from the proof of concept sound testing. From a repeated measure analysis of variance, the results show that there were statistically significant (at the 95% confidence level) reductions in both peak sound pressure and sound level from polymer integration. A post-hoc Duncan Least Significant Difference (LSD) measure was conducted for multiple comparisons of means.

These results indicate that metal-polymer impact surfaces produce less sound and vibration from the tool system. Furthermore, the greatest improvement was seen with the front insert where the piston impacts the chisel. As a result, the modeling and analysis that follows will focus on the development of a polymer interface between the piston and chisel. For simplicity and ease of prototyping, the polymer was modeled as a confined insert into the end of the chisel.

Table 1. Summary of preliminary power tool sound testing at 1 meter.
(signifies a statistical difference in means between the piston with a front polymer insert and the conventional piston; * † signifies a statistical difference in means between the piston with a back polymer disk from the other two test treatment.)*

Piston Treatment	Sound Pressure (Pa)	Sound Level (dBA)
Conventional Piston	41.7	126.6
Piston with Front Insert	23.8 *	121.8*
Piston with Back Insert	33.0 *+	124.5 *+

MODELING OF A CONFINED POLYMER INSERT

Nomenclature

E = elastic modulus
A = cross section area
t = polymer thickness in impact zone
k = cap stiffness
σ_x = stress on the chisel wall
σ_y = stress on the chisel wall, in the same plane but perpendicular to σx
σ_z = stress in the direction of the chisel shaft
ε_x = strain on the chisel wall
ε_y = strain on the chisel wall, in the same plane but perpendicular to εx
ε_z = strain in the direction of the chisel shaft
ν = Poisson's ratio
E' = constrained elastic modulus (effective modulus)

Methodology

Previous studies have reported several performance benefits from fitting a steel chisel with a polymer cap when compared to a conventional, hand-struck, bare chisel [6,7]. The impact between the metal piston and the metal chisel is the key area for design improvement considered within this study. Figure 6 illustrates an exploded view of a power tool chisel accessory with a polymer insert. A cylindrical insert was considered for simple integration with the existing shaft of the chisel. A hole bored into the top of the chisel allowed a cylindrical polymer plug to be pressed into the cavity created. By examining the mathematical relationships for polymer stiffness and axial compression, possible performance advantages for the confined insert configuration will be determined. Specifically, material property requirements of polymer modulus and Poisson's ratio will be considered for the selection of a reinforced polymer insert in confined compression.

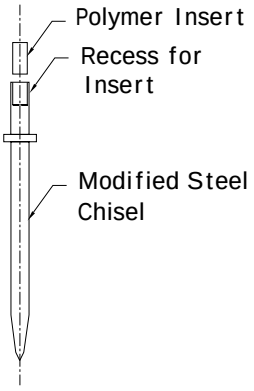

Figure 6. Exploded view of a steel chisel with a confined, reinforced polymer insert [13].

Design of a Polymer Insert

Previous work with polymer capped, hand-struck chisels demonstrated that the stiffness of the polymer must be high in order to transmit and exert high forces onto the target thus preserving tool performance [7]. Assuming the insert can be modeled as an axially loaded cylindrical plug of homogeneous isotropic material acting in the elastic range, the stiffness can be computed as:

$$k = E\,A\,/\,t \tag{1}$$

where,

E = polymer modulus
A = cross section area
t = polymer thickness in impact zone
k = cap stiffness

As expected, the polymer modulus must be high to insure high stiffness and peak impact force transmission. However, it is anticipated that the impact resistance must also be high to insure durability. Within the elastic limit of the material, there is a linear relationship between displacement and the force attempting to restore the material to equilibrium. Hooke's law defines the general relationship between stress and strain in the mechanics of materials,

$$E = \sigma_x / \varepsilon_x \tag{2}$$

The constrained compression on the polymer insert, illustrated in Figure 7, can be characterized by 3-D Hooke's Law for isotropic materials,

$$\varepsilon_x = \frac{1}{E}\left[\sigma_x - \nu\left(\sigma_y + \sigma_z\right)\right] \tag{3}$$

$$\varepsilon_y = \frac{1}{E}\left[\sigma_y - \nu\left(\sigma_x + \sigma_z\right)\right] \tag{4}$$

$$\varepsilon_z = \frac{1}{E}\left[\sigma_z - \nu\left(\sigma_x + \sigma_y\right)\right] \tag{5}$$

If constrained in x and y,

$$\varepsilon_x = \varepsilon_y = 0 \tag{6}$$

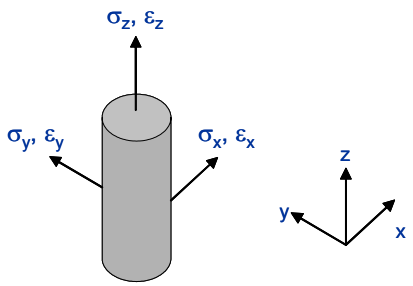

Figure 7. 3-D elemental representing the polymer insert.

and then,

$$\sigma_x = \nu\left(\sigma_y + \sigma_z\right) \quad (7)$$

$$\sigma_y = \nu\left(\sigma_x + \sigma_z\right) \quad (8)$$

and assuming uniform stress distributions on top of and around the cylinder, and for $\nu \neq 0$ then,

$$\sigma_z = \left(\frac{E\varepsilon_z}{1 - \frac{2\nu^2}{1-\nu}} \right) \quad (9)$$

The relation between zero radial strain and equal stresses in the planar directions parallel to the face surface of the insert yields an "effective" modulus E' for constrained polymer insert compression,

$$E' = \frac{E(\nu - 1)}{2\nu^2 + \nu - 1} \quad (10)$$

Note that the effective modulus is a function of the elastic modulus of the polymer material (E) as well as the volume change indicated by Poisson's ratio (ν). Both material property values for polymers of interest (Table 2) were obtained from Dupont Product Information Guides [8].

The imposed loading condition demonstrates that the confined polymer insert performance is not only dependent on material stiffness; the effective modulus is influenced by the directional deformation characteristics of the polymer. Figure 8 shows that higher Poisson's ratios demonstrate greater increase in effective modulus as a result of the confined insert design. Therefore, this confined (effective) modulus is much larger than Young's modulus for the simple unconfined insert compression, as illustrated in Table 2. It is anticipated that the higher apparent modulus of the confined polymer will provide significant advantages in terms of force transmission in the tool.

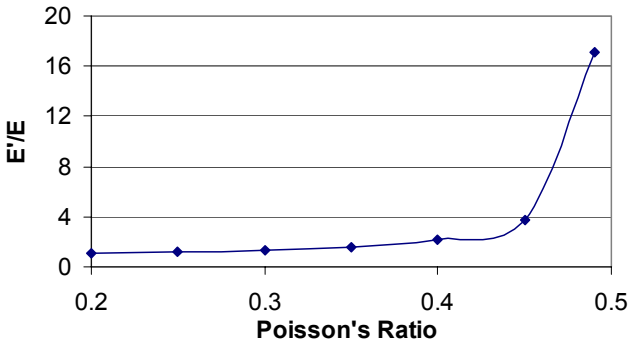

Figure 8. Normalized effective modulus vs. Poisson's ratio.

Table 2. Effective polymer modulus resulting from the confined insert configuration.

Polymer Material	Poisson's Ratio, n	Modulus (GPa) Rated	Effective	% Increase
Minlon™	0.40	5.2	11.2	114
Hytrel™	0.45	0.6	2.2	279

MODELING OF THE FORCE TRANSMISSION CHARACTERISTICS WITH A POLYMER INSERT

Nomenclature

x_1 = displacement of piston (from just touching back spring)
x_2 = displacement of chisel (from just touching "stop")
x_3 = velocity of piston
x_4 = velocity of chisel
x_a = piston reversal point
x_i = sharpness parameter
t_{sec} = time (sec)
m_1 = piston mass
m_2 = effective chisel mass
k_b = back spring
k_p = effective spring constant of piston and insert
k_{pa} = spring constant of entire piston
k_{pb} = spring constant of insert
k_{stop} = max stiffness of retaining spring
F_1 = reaction force on back of piston
F_2 = compressive force on top of chisel
F_p = compressive air force on back of piston
F_s = retaining spring force on chisel
F_w = reaction force of "work" being cut
F_R = residual force used to normalize forces (N)
L = length used to normalize lengths (m)
T = time used to normalize time (sec)
y_1 = dimensionless force on back of piston
y_2 = dimensionless force on front of piston
y_w = dimensionless force on work
y_p = dimensionless net pressure force on back of piston
y_s = dimensionless retainer spring force

Model Development

Figure 9 illustrates the key elements used in the spring-mass model of the impact tool system. The piston and chisel are the two specified masses. Stiffness of the piston, polymer, chisel, and "work" components are represented as spring elements. The permanent damage imparted by the tool on the work during each impact can be modeled as an energy loss from the system, E_w.

The analysis that follows was based on the following assumptions:

- There is a hard stop that limits chisel displacement back into the tool.

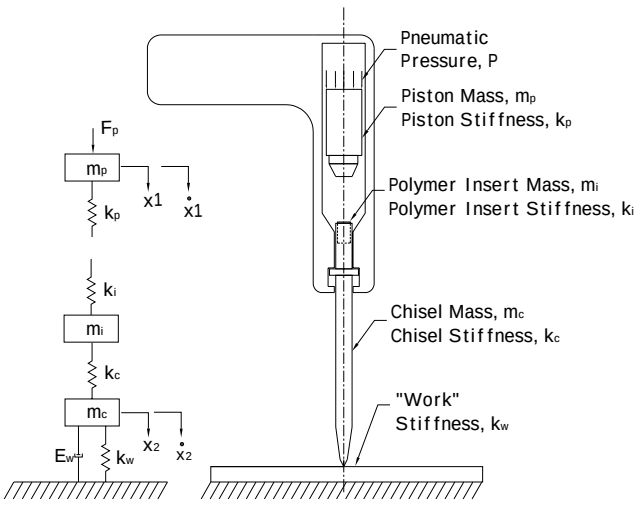

Figure 9. Mass and spring elements used to model the pneumatic tool impact system [13].

- Poisson's ratio and polymer modulus are not strain rate dependent.
- No coulomb friction or damping contributed to energy lost during component motion and impact.
- Deformations are linear elastic and energy is lost to the work, E_w, when the chisel is retracting from the work.

Mathematical Formulation

Summing the forces acting on each mass, the equations of motion for the piston and chisel are respectively,

$$F_1 = m_1\ddot{x}_1 + F_2 - F_P \tag{11}$$

$$F_2 = m_2\ddot{x}_2 + F_W + F_S \tag{12}$$

where the force due to the air pressure is,

$$F_P = \left(PA\tanh\left(\left(a - x\right)x_i\right)\right) \tag{13}$$

due to air pressure is modeled by a hyperbolic tangent because this function gives an abrupt change of direction of pressure force. The contact forces, retaining spring force, and reaction force due to the "work" being cut, respectively, are,

$$F_1 = MAX(-k_B x_1, 0) \tag{14}$$

$$F_2 = MAX(k_P\left(x_1 - x_2 - L\right), 0) \tag{15}$$

$$F_S = MIN(k_{stop}x_2, F_R + k_R x_2) \tag{16}$$

$$F_W = k_W x_2 \tag{17}$$

and the effective spring constant for polymer insert and steel chisel stiffness (i.e. two springs in series) is,

$$k_P = \frac{1}{\frac{1}{k_{Pa}} + \frac{1}{k_{Pb}}} \tag{18}$$

Combining the above equations gives the ordinary differential equations for the tool system with the specified boundary conditions,

$$\ddot{x}_1 + \frac{k_P}{m_1}\left(x_1 - x_2 - L\right) - \frac{PA}{m_1}\tanh((d - x_1)\xi) + \frac{k_B}{m_1}x_1 = 0 \tag{19}$$

$$\ddot{x}_2 + \frac{k_w}{m_2}x_2 + \left(\frac{F_R + k_R x_2}{m_2}\right) - \frac{k_P}{m_2}(x_1 - x_2 - L) = 0 \tag{20}$$

$$x_1(0) = x_2(0) = \dot{x}_1(0) = \dot{x}_2(0) = 0 \tag{21}$$

These equations can be normalized for computational simplicity. Defining the following,

$$T = \sqrt{m_2 / k_R} \tag{22}$$

$$F = Lk_R \tag{23}$$

$$a = F_R / F \tag{24}$$

$$b = PA / F \tag{25}$$

$$c = m_1 / m_2 \tag{26}$$

$$d = x_a / L \tag{27}$$

gives the dimensionless equations that describe the equations of motion of the piston and chisel illustrated in Figure 7,

$$\ddot{x}_1 + y_2 - y_P - y_1 = 0 \tag{28}$$

$$\ddot{x}_2 + y_W + y_S - y_2 = 0 \tag{29}$$

$$y_1(0) = y_2(0) = \dot{y}_1(0) = \dot{y}_2(0) = 0 \tag{30}$$

Simulation of the Piston and Chisel Motion and Forces

The differential equations were solved in vector matrix form using *Matlab*™ with initial conditions of zero state (no displacement, no velocity).

The following were identified as inputs to the model:

- Chisel modulus, top shaft diameter, length, density
- Piston weight, modulus, diameter, length
- Insert modulus, Poisson's ratio, diameter, length, density
- Spring constant of work
- Compressed air pressure

The outputs of the model were then defined as:

- Effective chisel weight
  [calculated from chisel and insert density and volume]

- Displacement vs. time for the piston
- Velocity vs. time for the piston
- Displacement vs. time for the chisel
- Velocity vs. time for the chisel
- Acceleration vs. time for the chisel
- Output force vs. time for the top of the chisel
- Output force vs. time for the bottom of the chisel
- Effective polymer spring constant
- Effective modulus for the insert
- Max force on the top and the bottom of the chisel

Most input parameters were determined by physical measurement. Only two parameters – the sharpness factor of the hyperbolic function and delta, the ratio of air flow reversal point to total piston stroke length – were chosen to ensure complete reciprocating motion of the piston (values of 100 and 0.6, respectively). The complete set of simulation parameters are documented in Table 3. Insert diameter and insert length are specified as design variables of choice. Figure 10a is the pressure function used in the model (i.e. Equation 13). Figures 10b through 10d are typical time graphs of simulation outputs for one impact cycle with the prototype chisel with a polymer insert.

Table 3. Parameter values used in simulations.

Parameter	Value used in Simulations
Piston Weight	93.0 g
Piston Diameter	1.89 cm
Piston Length	4.60 cm
Piston Stroke Length	5.96 cm
Chisel Top Shaft Diameter	1.01 cm
Effective Chisel Length	24.8 cm
Insert Diameter	Design Variable
Insert Length	Design Variable
Steel Density	1.0E-06 N/m^3
Steel Modulus	206.9 GPa
Minlon™ 11C40 Density	2.0E-07 N/m^3
Minlon™ 11C40 Modulus	5.2 GPa
Minlon™ 11C40 Poisson's Ratio	0.40
Hytrel™ 7246 Density	1.7E-07 N/m^3
Hytrel™ 7246 Modulus	0.57 GPa
Hytrel™ 7246 Poisson's Ratio	0.45
Kr, Retaining Spring Constant	25 kN/m
Kw, "Work" Spring Constant	87563 kN/m
Fr, residual spring force	30.6 N
Compressed air pressure	621 kPa

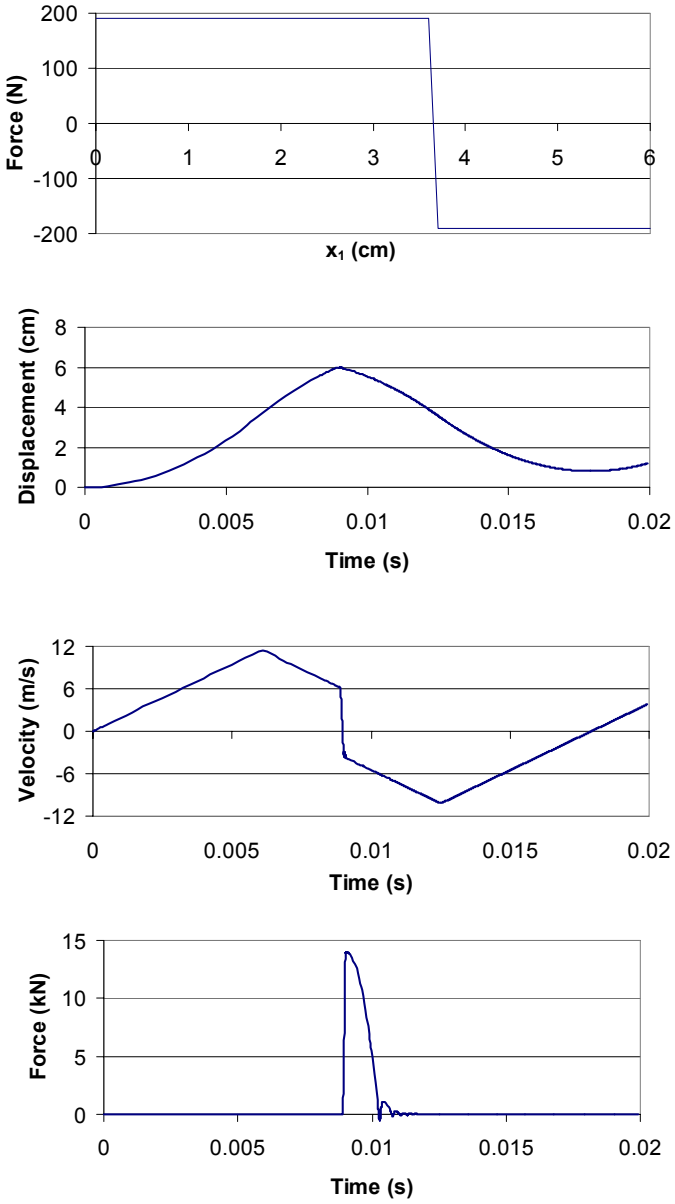

Figure 10. Model pressure function input (a), piston displacement (b), piston velocity (c), and chisel output force (d) for one impact cycle.

Prediction of Chisel Cutting Force During an Impact

Table 4 summarizes the results of simulated force for the top and the bottom of the chisel. In each case, the forces shown are for both a conventional chisel and a chisel with a polymer insert. For the chisel with a polymer insert, the insert has been modeled with a geometry of length L = 1.5 centimeters and diameter d = 0.72 centimeters. The force on the bottom is most relevant since it is the force actually cutting into the work. The slight difference seen in the simulated force values between the top and bottom of the chisel demonstrates the effect of the chisel inertia. While chisel inertia slightly

reduces predicted values of force transmission between the top and bottom of the chisel in both scenarios, the maximum chisel forces for the conventional chisel are only slightly higher than the forces predicted for the chisel with a constrained Minlon™ polymer insert. Force vs. time is plotted on Figure 11 for the force at the bottom of the chisel.

Table 4. Summary of maximum predicted forces for various chisel configurations. For the chisels with a polymer insert, the insert has been modeled with a geometry of L = 1.5 centimeters and d = 0.72 centimeters.

Chisel Treatment	Force at Top of the Chisel (kN)	Force at Bottom of the Chisel (kN)
Conventional Steel Chisel	17.00	16.99
Chisel with Minlon™ Insert	14.11	13.92
Chisel with Hytrel™ Insert	6.18	6.08

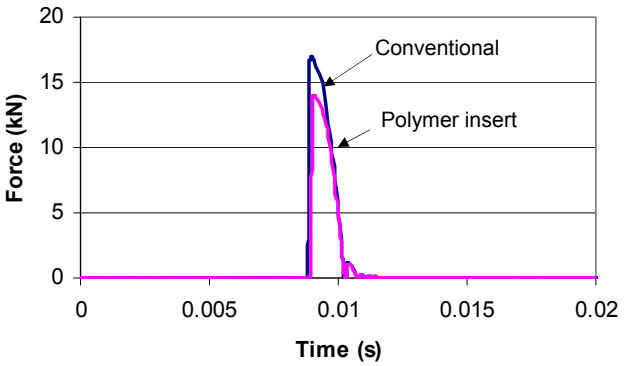

Figure 11. Predicted force vs. time for the force at the bottom of conventional and polymer insert chisels.

Effect of Polymer Properties on Maximum Output Force

Maximum chisel force is the key parameter for tool performance, therefore, the polymer modulus-force relation has been examined. Higher modulus polymers yield higher effective modulus values (Table 2). It is expected that increasing the effective polymer modulus will increase the maximum chisel force achieved. Maximum force is plotted against the polymer modulus normalized by the modulus of steel in Figure 12. Constrained compression increases the effective stiffness of a polymer which leads to an increase in output force.

Two key conclusions were drawn based on this evaluation. First, the modulus of high impact polymer materials can be increased by constraining inserts within the chisel housing. Second, polymer inserts with a high effective modulus produce a maximum output force that is close to that of a conventional chisel accessory. The more stiff and incompressible a polymer material, the greater the maximum chisel force. However, possible design tradeoffs do exist between insert stiffness,

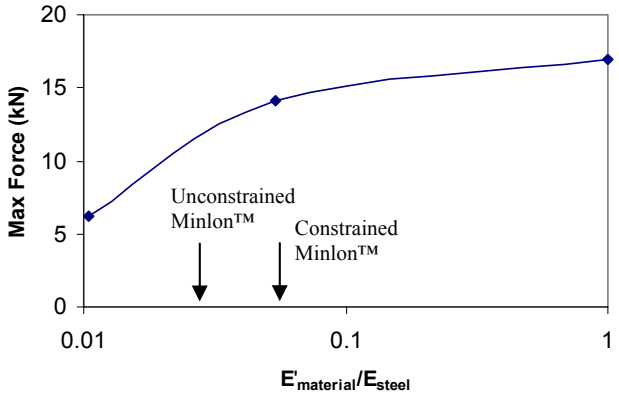

Figure 12. Effect of insert modulus on the maximum predicted chisel force.

reduction in vibration transmission, and desired insert durability.

Model Validation

Laboratory testing was used to validate the accuracy of the force predictions. A 44 kN capacity load cell was used to quantify the peak force exerted on a 6.35 mm drill rod by the cutting tool. Table 5 compares the predicted maximum output force exerted by the chisel to the measured value of force. The measured values of force for both a conventional chisel and a chisel with a polymer insert are similar to the simulation results. As expected, the mean value results show that a polymer insert reduces chisel force, however, this reduction was found to be statistically insignificant (at the 95% confidence level).

Table 5. Summary of predicted and measured force exerted on the test specimen by the chisel. There was a small but statistically insignificant decrease in measured force output for a prototype chisel when compared to the output force value for a conventional chisel.

Treatement	Predicted Force (kN)	Measured Force (kN) 95% LB	Mean	95% UB
Conventional Steel Chisel	16.99	14.94	16.10	17.28
Chisel with Insert	13.92	10.68	14.30	17.83

Effect of Polymer Insert Diameter and Length

Increasing polymer stiffness certainly increases chisel force. For the conventional chisel system, the model predicted a maximum output force of 17 kN. From Equation 1, it is expected that polymer stiffness can be improved by increasing insert diameter (which increases cross sectional area). It is also anticipated from this equation that increasing insert length reduces insert stiffness.

The effect of polymer insert length was computed and is shown in Figure 13. The zero insert length corresponds to a conventional chisel. As expected, increasing polymer length decreases maximum force. Longer polymer inserts are not as stiff as shorter inserts of the same diameter.

The effect of insert diameter on various insert lengths (Figure 14) results in a relation similar to the modulus effect predicted on Figure 12. Maximum chisel cutting force increases as insert diameter increases and insert length is reduced. In other words, as the geometry of the insert increases polymer stiffness, the exerted output force from the chisel is higher. The zero insert diameter level corresponds to the maximum force output of a conventional chisel.

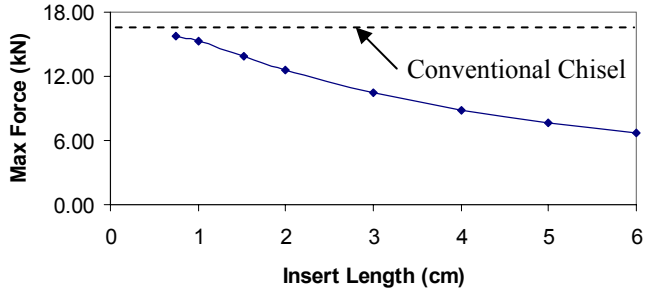

Figure 13. Predicted maximum force for a chisel with a polymer insert vs. insert length for an insert diameter of 0.72 cm.

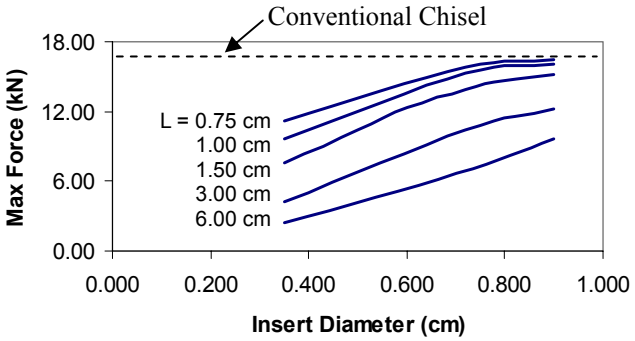

Figure 14. Predicted effect of insert diameter and length on peak chisel with a polymer insert.

DURABILITY AND PERFORMANCE TESTING

Methodology for Insert Integrity Testing

Two methods of testing are described. Laboratory testing using a materials test machine (Instron™ Model 1331 High Frequency Servohydraulic Test Machine with a Series 2150 controller) is performed to artificially age the polymer insert with repeated loading cycles. Test results are used to confirm the effective modulus of the insert and understand the life-load behavior (i.e. the durability) of the polymer insert. In addition, field (human) trials in which a pneumatic chisel equipped with a chisel and polymer insert are conducted to measure the

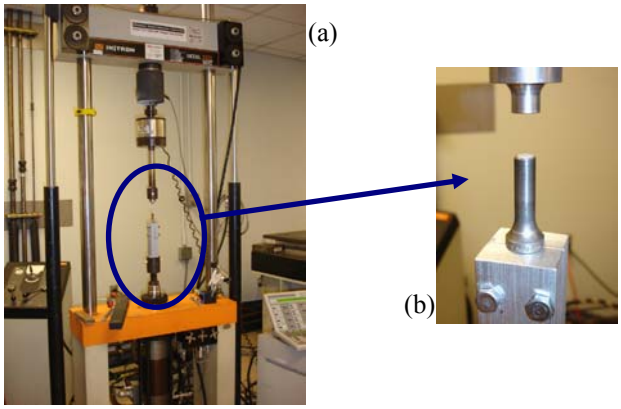

Figure 15. The prototype chisel is held in a fixture during Instron™ machine laboratory testing (a). The top of the chisel remains exposed (b) for all tests.

vibration and sound emission characteristics of the new tool. Prototype chisels were mounted in the high frequency materials testing machine shown in Figure 15. The top portion of the prototype chisel was exposed when mounted for testing. The testing machine applied a regular sinusoidal load cycling between 0.89 kN and 12.5 kN at 15 Hz for one million cycles. Modulus values were estimated from load-deformation data.

Measured Insert Stiffness (Modulus)

Tests were conducted with a chisel and new Minlon™ insert and a chisel with a Minlon™ insert aged by loading. Figure 16 shows a typical stress-strain plot for a chisel with a new Minlon™ insert. The average computed modulus for 10 measurement trials for each insert test condition is summarized in Table 6. Analysis of variance for the results show that there was a small but significantly insignificant increase (at the 95% confidence interval) in the insert stiffness for the artificially aged insert. Photographs of the top of the chisel with a polymer insert prior to Instron™ aging and after Instron™ aging are shown in Figure 17.

The experimental technique and methodology used to artificially age an insert with the materials testing machine is accurately controlled and yields repeatable results. While aging did not significantly increase the stiffness of the polymer insert, the cyclical loading did contribute to the survivability of the insert during later tool use. Experimental testing of prototype chisels that were used in a tool without aging (initial repeated loading) resulted in the quick disintegration of unconfined polymer material. As a result of artificially aging a chisel with a polymer insert, the prototype chisel survived running in the tool (no cutting) for 1 hour of time. While the exposed polymer is slightly compressed as a result of the combination of aging and 1 hour of tool use, the inverted conical frustum shape of the exposed insert remains preserved as seen in Figure 18. Three speculations for beneficial performance of the insert after cyclical loading in the materials testing machine have been proposed. The simplest explanation is that plastic flow could occur into the conical bottom of the

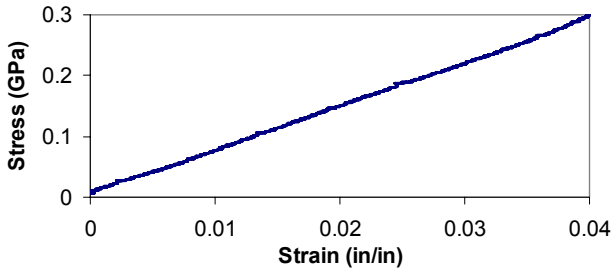

Figure 16. Typical stress-strain graph of new, constrained Minlon™ insert in the chisel.

Table 6. Summary of measured polymer insert modulus values for 10 trials. Averages and the range of responses are given.

	New Insert	Preloaded Insert
Modulus (GPa)	6.94 (6.27 to 7.24)	6.86 (5.83 to 7.52)

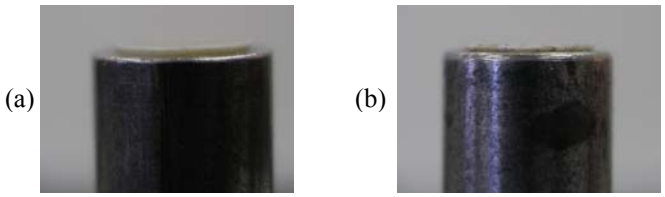

Figure 17. Photographs for the top portion of a prototype chisel with a Minlon™ insert (a) prior to Instron™ testing and (b) after pre-cycling.

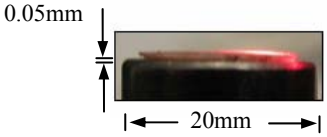

Figure 18. Top portion of a prototype chisel with a Minlon™ insert after Instron™ preloading and 1 hour of tool use. The length of exposed polymer prior to preloading was 0.10 cm.

drilled chisel cavity. A second consideration is possible creeping of the insert due to friction, preventing the polymer from fully recovering after loading. Finally, a change in crystalline structure of the insert during loading may straighten and align bonds between polymer chains.

Instrumentation and Data Acquisition & Analysis for Vibration and Sound Emission Measurements

Vibration measurements were made at the pneumatic chisel handle-hand interface using a PCB Piezotronics Tri-Axial Accelerometer (Model SEN021F) with a nominal sensitivity of 10 mV/g and a frequency response range of 1-10000 Hz. A small mounting fixture was used to position the accelerometer along the hand. Signal conditioning was perfomed with a PCB Piezotronitcs Model 480B21 Three-Channel Conditioner. A LinearX 150 mm diameter precision acoustic measurement microphone (Model M51A) with an acoustic sensitivity of 11.086 mV/94.00 dBspl was used for all tests. A DC supply of 9 volts powered the calibrated microphone and a National Instruments Data Acquisition Card (E-Series, PCMCIA 16-bit) and laptop computer were used to record the sound signal along with the vibration signals.

A *LabVIEW* program was written to interface to the A/D board and collect data as well as process, analyze and log the acquired signals (Figure 19). The averaged level of the sound pressure signal was computed based on an exponential mode after each sample of time and returned as an exponential averaged sound level in decibels. Selecting a custom exponential time constant of 125 milliseconds allowed for the continuous running average to accurately capture a short duration impulsive signal. Discrete Fourier transforms of the sound pressure and acceleration were performed using the following form:

$$F_n = \sum_{k=0}^{N-1} f(n) e^{i 2\pi n k / N} \qquad (31)$$

where,

F_n = Fourier transform
$f(n)$ = n^{th} measured time domain data
N = Number of data

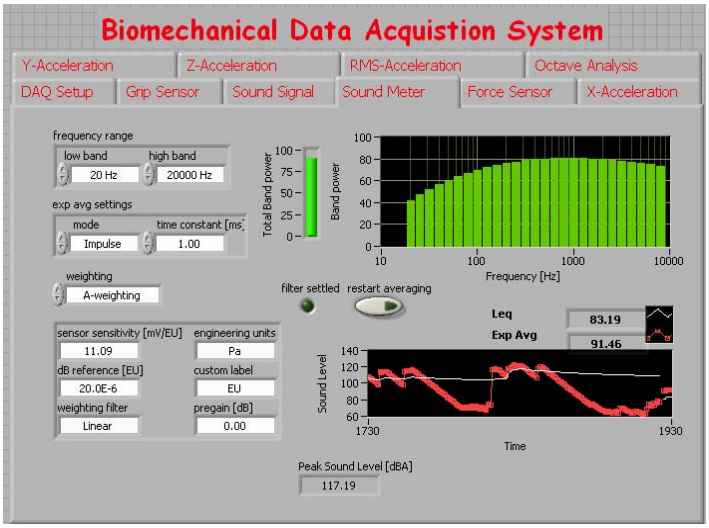

Figure 19. *LabVIEW* interface for the data acquisition and processing program used to collect and analyze the sound and vibration data.

Analysis of Tool Sound Emission

The results of quantitative sound measurement recorded in decibel readings are summarized in Table 7. Averagesresponses are given for sound at a 1 meter distance.

Using a repeated measure analysis of variance, the chisel with a polymer insert was found to significantly reduce the continuous running average (Leq) and exponential running average (Exp) of sound emission by the tool system. However, a statistically insignificant reduction in peak sound pressure (dBA) was recorded for the chisel with a polymer insert when compared to the conventional steel chisel.

Figures 20 and 21 contain typical sound pressure vs. time plots for a pneumatic tool with a conventional chisel and chisel with a polymer insert, respectively. Analysis of the frequency content of these signals illustrated in Figures 22 and 23 suggests that a chisel with a polymer insert reduces the sound emitted by a pneumatic chisel across the frequency spectra, including harmful high-frequency noise.

Table 7. Summary of sound testing for a chisel with a Minlon™ preloaded insert and a conventional chisel. (*signifies a statistical difference in means).

Chisel Treatment	Leq* (dBA)	Exp * (dBA)	Peak Pressure (dBA)
Conventional Steel Chisel	108.8	106.6	126.9
Chisel with Insert	106.6	104.4	125.3

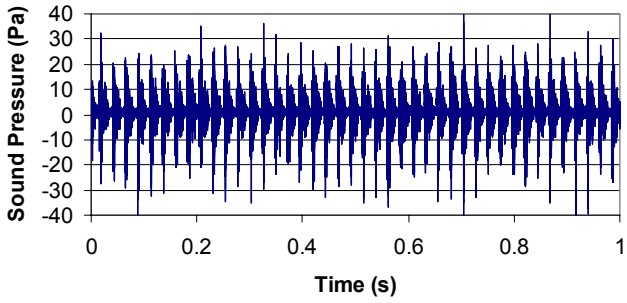

Figure 20. Typical time domain response of sound for a conventional chisel.

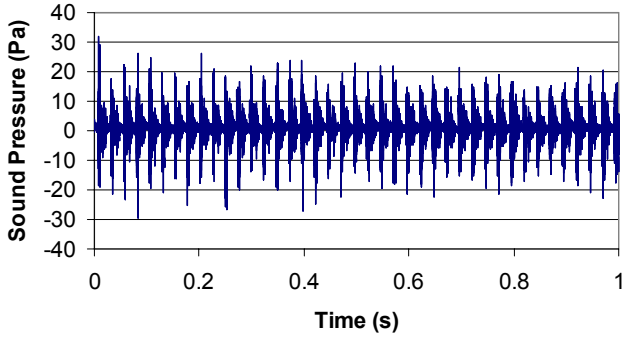

Figure 21. Typical time domain response of sound for a prototype chisel with a Minlon™ insert.

Analysis of Tool Vibration

To measure the vibration transmitted to the hand that was holding the pneumatic tool, the triaxial accelerometer was mounted on the tool at the hand-handle interface. Tests were conducted with a prototype polymer insert chisel in the pneumatic tool illustrated in Figure 4; measurements were

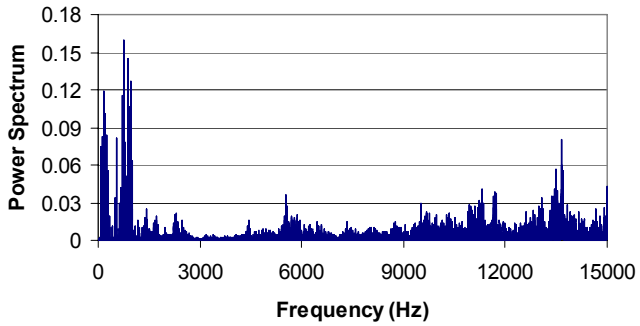

Figure 22. Frequency spectra of the sound pressure data in Figure 20 for the conventional chisel.

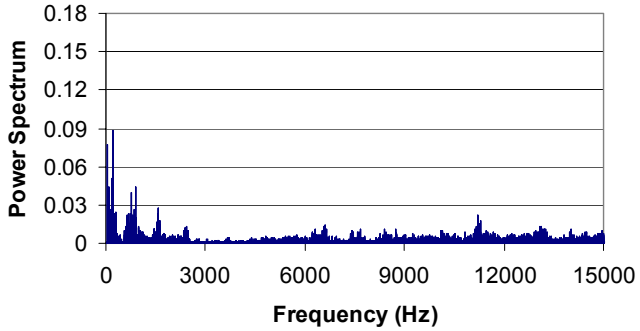

Figure 23. Frequency spectra of the sound data in Figure 21 for a prototype chisel with a Minlon™ insert.

made with the tool cutting a 6.25 mm steel drill rod. A conventional chisel without an insert was also tested as an experimental control. In general, vibration magnitudes were greatest in the axial direction (i.e. the direction of cutting) for all tests. Figures 24 and 25 contain typical axial acceleration vs. time plots at the tool-hand interface for a conventional chisel and a chisel with a polymer insert, respectively. Examination of these graphs revealed that vibration in the axial direction was reduced by a factor of 2. The axial direction is the direction in which the tool and piston travel, and was the predominate direction of vibration in all tests.

For both the conventional and prototype chisel, there was significant high frequency content associated with the tool between 4,000 and 6,000 Hz as illustrated in Figures 23 and 24. Although the chisel with a polymer insert did not seem to shift this regime of vibration to a lower frequency, the prototype chisel did reduce the magnitude of the power spectrum. The low frequency vibration in Figures 26 and 27 corresponds to the impact frequency of the internal piston component (rated at 58 Hz). The chisel with a polymer insert did reduce the magnitude of accelerations at this low frequency as well.

To determine the effects of the insert on vibration transmitted in the arm, tests were conducted in which measurements were made at the elbow. The triaxial accelerometer was mounted on the user's elbow using a small mounting fixture and zip ties. In all tests, the predominant magnitude of vibration was in the lateral direction, where lateral is defined as the medial lateral direction in the coronal plane. Figures 28 and 29 contain typical lateral acceleration vs. time at the elbow while using the conventional and polymer insert chisels, respectively. The corresponding frequency spectrums for each tool configuration are provided in Figures 30 and 31. Like the measurements taken at the hand, vibration levels at the elbow were reduced with the polymer. However, power spectrums for both the conventional and polymer chisels reveal that only a single dominant frequency is present corresponding to the cycle frequency of the piston. Surprisingly, it appears that no high frequency components of vibration present at the hand (evident in Figures 26 or 27) are transmitted to elbow for either tool suggesting that most of vibration energy is absorbed in the hand and wrist.

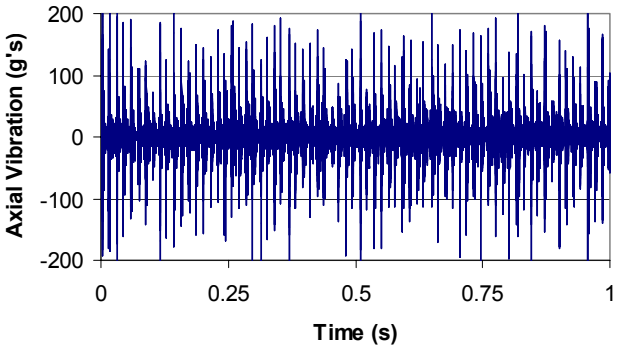

Figure 24. Typical time domain vibration response in the axial direction at the *hand* for a conventional chisel.

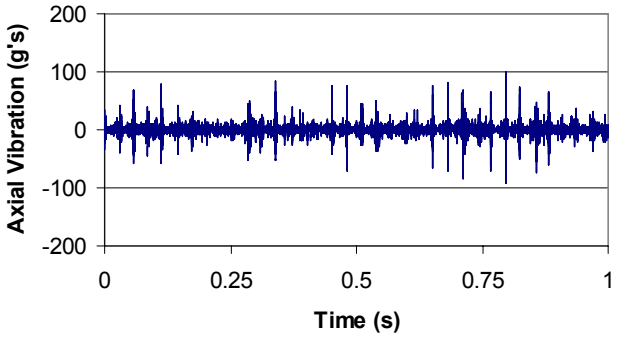

Figure 25. Typical time domain vibration response in the axial direction at the *hand* for a prototype chisel with a Minlon™ insert.

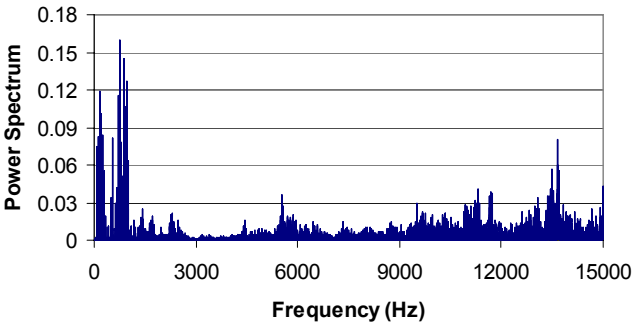

Figure 26. Overall frequency content of the data in Figure 24 for a conventional chisel.

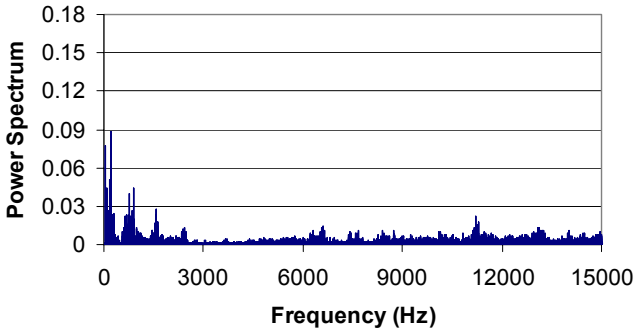

Figure 27. Overall frequency content of the data in Figure 25 for a prototype chisel with a Minlon™ insert.

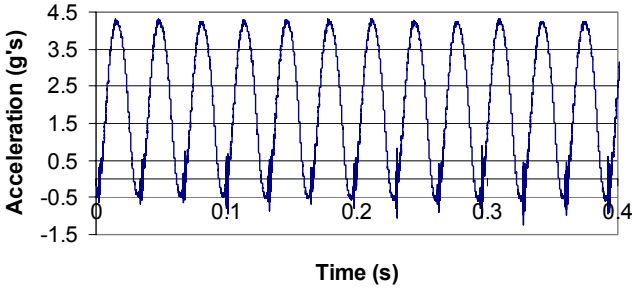

Figure 28. Typical time domain lateral vibration response at the *elbow* for a conventional chisel.

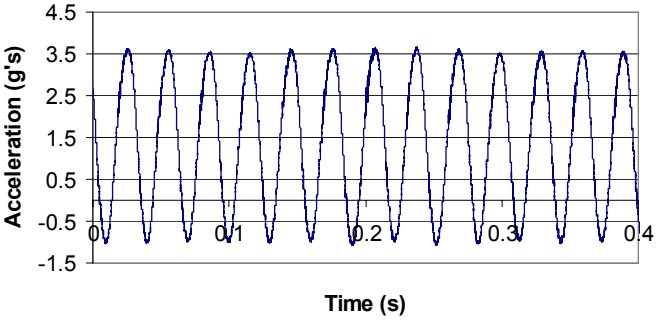

Figure 29. Typical time domain lateral vibration response at the *elbow* for a prototype chisel with a Minlon™ insert.

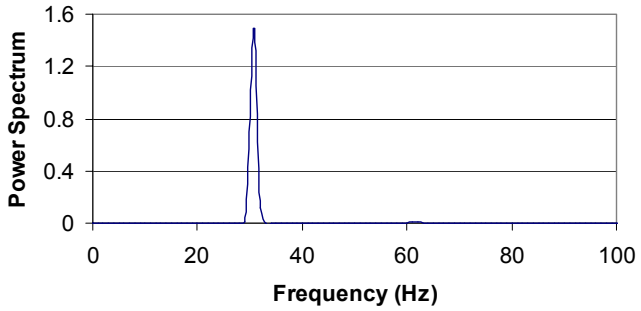

Figure 30. Overall frequency content of the data in Figure 28 for a conventional chisel.

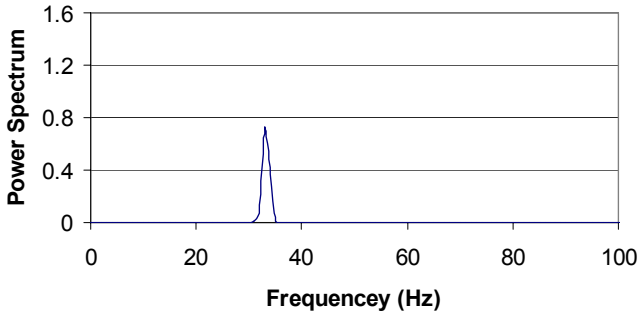

Figure 31. Overall frequency content of the data in Figure 29 for a prototype chisel with a Minlon™ insert.

General Discussion and Future Work

Conventional chisels and their cutting accessories produce high levels of sound that have the potential to damage the ear along with magnitudes and frequencies of vibration that contribute to biomechanical injuries over time. The test results from this study are encouraging since both low and high frequency components of vibration are being reduced by the polymer insert. This is especially important at the lower frequencies where the most blood vessel and nerve damage is believed to occur from long term exposure to continuous vibration. Other studies for vibration transmission through the human arm have shown that lower frequency vibration (<50 Hz) is transmitted with little attenuation along the hand and forearm with most vibration energy above 150 to 200 Hz dissipated in the tissues of the hand and fingers [9]. This has been demonstrated with the effects of the insert on vibration transmitted to the hand and arm. In addition, a polymer insert also produces significantly less noise across the frequency spectra, including harmful high-frequency sound components that are most prone to induce permanent damage to the hair cells lining the cochlea within the ear.

The parameters of polymer modulus and Poisson's ratio effect the selection of an appropriate reinforced polymer for a chisel insert. Confining a polymer insert created a hydrostatic compressive loading condition, thus increasing the polymer apparent modulus of elasticity and improving force transmission characteristics. While no significant increase in measured stiffness resulted from artificial aging of a chisel with a polymer insert, cyclical loading in a materials testing machine was found to increase the survivability of the polymer material during tool operation. A study of high strain rate impact testing and evaluation of finite element modeling should be initiated for evaluation of polymer insert durability and vibration energy transmission characteristics, respectively. With a fundamental understanding of the durability benefits gained from pre-cycling, choice of a better reinforced polymer material for the insert application may eliminate the additional processing step currently required in the materials testing machine.

CONCLUSIONS

1. Properly designed polymer inserts in power impact tools significantly reduce noise and vibration, but not impact force.
2. Optimum geometry for a polymer insert is a cylindrical plug in a cavity of the piston or cutting tool such that the polymer is loaded in confined compression.
3. An effective material for a polymer insert that meets the requirements of high modulus as well as high toughness is a mineral reinforced nylon.
4. A mathematical model consisting of several non-linear differential equations adequately described the mechanics of a power impact tool. The model was also able to predict tool performance with a polymer inserted into the impact mechanism.
5. After assembling the polymer insert into the cavity in the tool, performance is improved greatly by cyclical preloading.
6. Power impact tools with polymer inserts have the potential to significantly reduce hand and arm injuries by reducing vibration exposure to the user. In addition, lower sound pressure levels emitted from this design may also reduce the potential for hearing loss.

ACKNOWLEDGMENTS

The authors would like to acknowledge Harry "Downie" McCarty, President of Baltimore Tool Works, Inc., for his support throughout this project. The authors would also like to thank Rick Tobar and Marc Wichmann from Dupont Engineering Polymers for their technical assistance, and for providing material samples for testing.

REFERENCES

[1] United States Department of Labor, Bureau of Labor Statistics. 2004. Survey of Occupational Injuries and Illnesses in cooperation with participating State agencies. U.S. Bureau of Labor Statistics Postal Square Building, 2 Massachusetts Ave., NE, Washington, DC 20212-0001

[2] United States Navy, Navy Safety Center. Acquisition Safety Vibration. Naval Safety Center, 375 A Street, Norfolk, VA 23511

[3] United States Department of Labor, Occupational Safety & Health Association, (1999). Proposed Ergonomics Program, Federal Registrar #64:65768-66078. U.S. Department of Labor Occupational Safety & Health Administration, 200 Constitution Avenue, Washington, D.C. 20210.

[4] The Health and Safety Executive (HSE), Hand-Arm Vibration – Advice for Employees. Publication No. INDG296(rev1). Health and Safety Executive, Rose Court, 2 Southwark Bridge, London, SE1 9HS

[5] Barab, J. 2002. Lies, Partisanship Caused Ergo Standard to Crumble. Safety and Health Magazine, February, 2002.National Safety Council, Safety and Health, 1121 Spring Lake Drive, Itasca, IL 60143-3201

[6] Glancey, J.L., J. Moore, D. Muhlenforth, J. Lawrence, (2004). Measurement of Manual and Power Impact Tool Vibration Transmission to the Hand. Paper No.047027. Written for Presentation at the 2004 ASAE/CSAE Annual International Meeting, Ottawa, Ontario, Canada.

[7] Glancey, J.L., P. Popper (Dupont), T. Nasr, P. Truitt, M. Orgovan, D. O'Brian, (2003). Design and Performance of Hand-Struck Impact Tools Using High Performance Engineering Polymers. Paper No. IMECE2003-41455. Proceedings of the 2003 ASME International Annual meeting, Washington, D.C.

[8] The Dupont Co., 2006. Product Information, Dupont Minlon 11C40 NC010. Product Sheet No. 050722. The DuPont Co., Wilmington, DE.

[9] Bovenzi, Massimo. 2006. Hand-Transmitted Vibration. Encyclopedia of Occupational Health and Safety, 4th Ed. International Labour Office 4, route des Morillons CH-1211 Geneva 22 Switzerland.

[10] Glancey, J.L., P. Popper, J. Moore, D. Muhlenforth, and T. Nasr. 2004. Modeling and Experimental Evaluation of Hand and Power Tools Vibration Transmission to the Hand and Arm. ASAE Paper 047027. ASAE, 2959 Niles Road, St. Joseph, MI 49085-9659.

[11] International Standards Organization. 1986. ISO Standard 5349: Mechanical vibration – Guidelines for the measurement and assessment of human exposure to hand-transmitted vibration, International Organization of Standards, Geneva, Switzerland.

[12] Glancey, J.L., P. Popper (Dupont), M. Mitch, P.Truitt, T. Nasr, M. Orgovan, J. Stevens. 2003a. A new cyclic impact device and standard testing methodology for hand struck tools. Paper No. IMECE2003-41451. Proceedings of the 2003 ASME International Annual Meeting, Washington, D.C.

[13] Konchar, J. 2006. Mathematical modeling and testing of a new polymer-based impact tool design to reduce vibration-related biomechanical injuries. Degree with Distinction Thesis, University of Delaware, Newark, DE.